عدد خاص
بالمؤتمر الليبي الدولي للعلوم التطبيقية
و الهندسية
27-28- سبتمبر 2022

Study the effect of some attributed process parameters in riveting for the sequence, the distance between rivets, and the gap between the aluminum alloys sheets 2024

Khaled Aljaly [1], Ismail. M. Balaid[2], Mohamed. R. Budar[3], Faouzi Masmoudi[4]

[1] Afriqiyah Airways Company
Corresponding author: kaljaly0@gmail.com
[2] Technical and Research Centre
[3] College of Engineering Technology-Janzour
[4]Mechanics, Modelling, and Production Research Laboratory, Mechanical Department, National
School of Engineering of Sfax, University of Sfax, Sfax, Tunisia

Abstract

In this paper, some process parameters which are disturbed in the clamping distance between screws and the gap between the aluminum alloy plate 2024 on the quality of the screws were studied. Where in this study the focus was on a flat-head rivet with a diameter of 3.175 mm and a thickness of 1.5 mm. And a sheet of aluminum alloy type 2024. A type simulation program ANSYS (16) was selected for the variables of the riveting process as modeling and analysis of the riveting process, which was statistically performed. A comparison was made between experimental and simulated experiments. The results showed a good combination of simulation and experiment, as well as low values of residual stresses on plates, nails, and swelling, which reduces the chances of clearance after installation in the riveted roll joint.
Keywords: Rivet, aluminum alloy, finite element simulation.

الملخص

في هذا البحث تم دراسة بعض المعلمات للعمليات والتي تتنثل في مسافة التثبيت بين البراغي والفجوة بين صفيحة سبائك الألومنيوم 2024 على جودة البراغي. حيث تم في هذه الدراسة التركيز على برشام برأس مسطح بقطر 3.175 مم وسمك 1.5 مم.و صفيحة من سبائك الألومنيوم نوع 2024. تم إختيار برنامج محاكاة ANSYS (16) نوع لمتغيرات عملية البرشمة كنمذجة وتحليل لعملية التثبيت حيث تم إجراؤها إحصائيًا.تم إجراء مقارنة بين التجارب العملية والمحاكة. حيث اظهرت النتائج المزيج الجيد بين المحاكاة والتجربة كما اظهرت قيمًا منخفضة للاجهادات المتبقي علي الألواح والمسامير والانتفاخ مما يقلل من فرص الخلوص بعد التثبيت في مفصل اللفة المبرشمة.
الكلمات الدالة: برشام، سبائك الالومنيوم، المحاكاة.

1. Introduction

Riveting is a commonly used process of joining aluminum. When carried out, riveting can produce extremely dependable and consistently uniform joints without affecting the strength or other characterized sites of the metal. However, it is more time-consuming and creates bulkier joints than those made by other joining methods. Also, riveting requires care in the formation of holes rivets, in the selection the size and length of the rivet, and the choice of its material and temper. In addition, the

selection of rivet size is not governed by hard-and-fast rules so that the diameter and the length do not be damaged during the riveting process, and that leads to a good joint of the rivet. In general, the diameter must be greater than the thickness of the thickest part through which the rivet is installed [1].

Accepting the rivet without forcing the holes must be adequate and that will not lead to the bending of the rivet, or the sheets will bulge or separate. Also, the holes should be small enough so that the rivets will be fitted without excessive cold work [2]. The distance between the holes should be such that the sheets are not weakened by the holes, and that the sheet does not buckle. According to (Uhe, Benedikt et al., 2020) the spacing (center-to-center) should be not less than three times the hole diameter nor more than 24 times the thickness of the sheet. Holes for riveting may be formed by punching, drilling, or by sub punching and reaming. Drilling is preferred to punching because it does not produce rough edges which might cause cracks to propagate radially from the hole [3].

The choice of rivet material is controlled by several considerations including :corrosion problems, property requirements, and fabricating costs. From a strength point of view, it is generally advantageous to use a rivet which material has the same properties as the base material [4].

2. Experimental setup

Two identical plates were riveted together by fastening two rivets through both plates as shown in Figure 1.

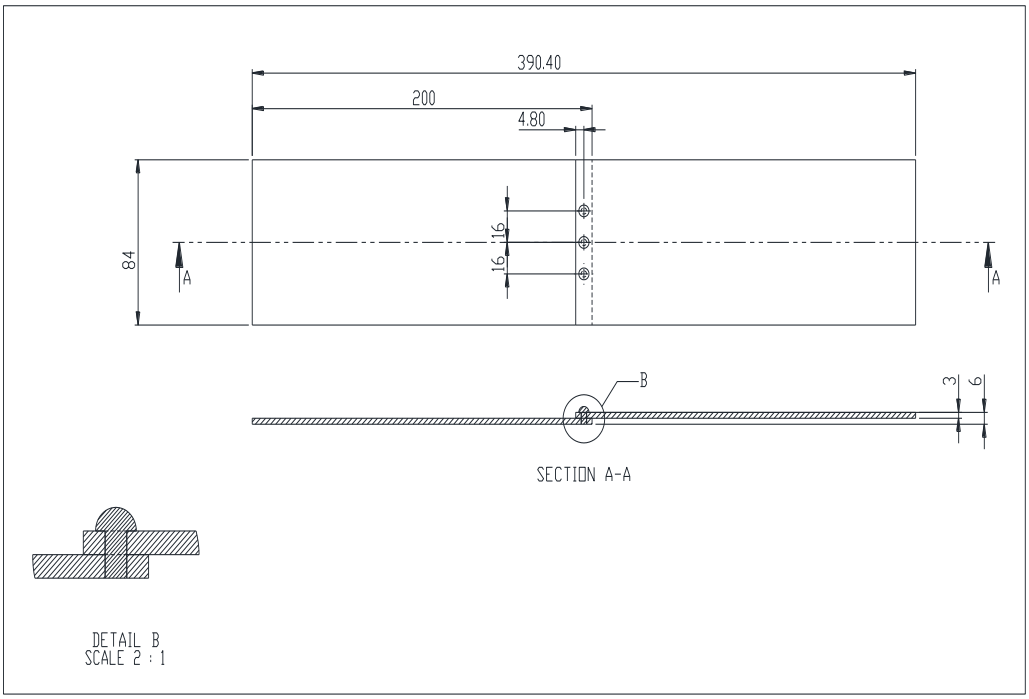

Figure (1): Bolted joint specimens double bolt joint.

The riveted aluminum 2024-T3 panels along the longitudinal axis were parallel to the rolling direction. Plates of thickness 2 mm was drilled using a drill bit of d = 6.5 mm in the center of the specimen with side free margins of e = 9.5 and 12.7mm. Diameter of aluminum rivets (grade 2117) were used to clamp the specimen couples and apply a tightening torque of 10 N/m using a digital torque wrench.

Table (1): Material Properties of Aluminum Alloy 2024 T4 and Rivet 2017 T4

MATERIAL	YOUNG, S MODULUS	POISSON, S RATIO
Aluminum 2024 T4 (SHEET)	**74 GPA**	**0.33**
Aluminum 2117 T4 (RIVET)	**71.7 GPA**	**0.33**

Figure 2 shows the complete finite element analysis of a riveting joint model with symmetric loading and geometry conditions on the XY and YZ planes. The displacement boundary conditions were applied to the nodes on the cut planes.
Quadratic hexahedral elements (C3D8R) were used for meshing the model. As near the bolt hole, the analysis must be carried out at the critical zone and the density of the mesh was appropriately refined in this region.

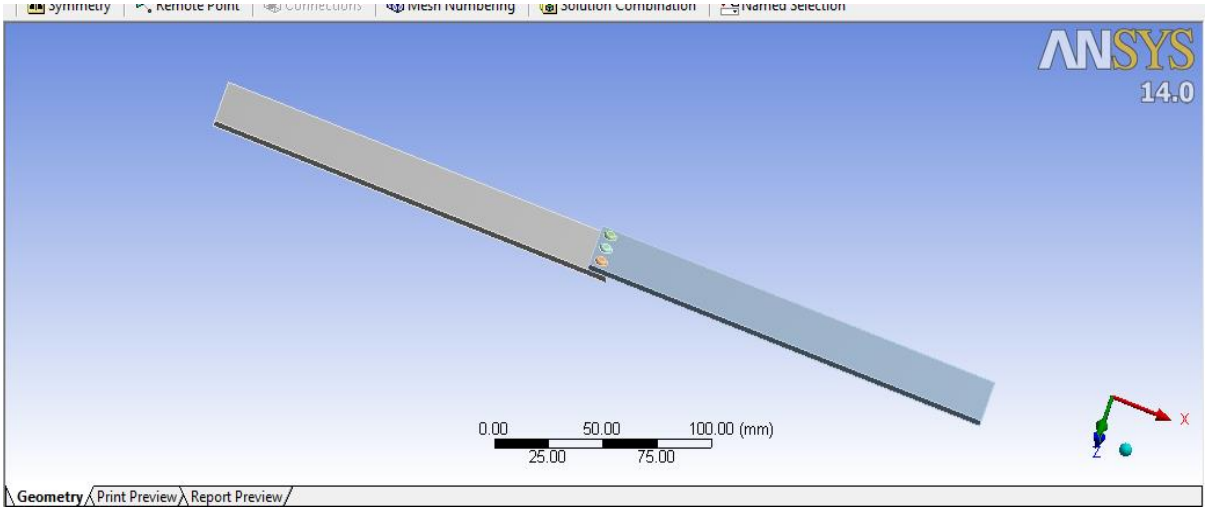

Figure (2): Finite element model of the bolted joints.

The contact between the plates such as the bolt, and inside the hole and washer were successfully implemented using a finite sliding formulation with a surface-to-surface discretization method. A Lagrange multiplier formulation was used to represent the contact pressure in a mixed formulation of pressure and contact surfaces. A penalty friction formulation was used with friction coefficients of 0.23, 0.35, and 0.25.
Between the plates and the screw shank and washer or top plate, there is a space. The coefficient of friction between the contacting parts was obtained by experiments based on the sliding of a small piece of each part under its weight on the inclined surface of an aluminum plate. It should be noted that the friction coefficient may not be constant and may vary in the joint under mechanical load [6-7]. However, in this study, the coefficients of friction were assumed to

remain constant during the loading process. A good fit was found between the simulation results and the experimental data in this study

4. Experimental work

Verification of Finite Element Model was achieved by comparing joint specimen data on load-displacement obtained from experimental and numerical methods until the displacement reached 4 mm. The results were very good and the maximum applied load was found to be less than 6% greater than the maximum allowable applied load.

The rivet and aluminum alloy sheets are materials that undergo plastic deformation, which is modeled using an isotropic plasticity model with rate effects. The power hardening rule is used to calculate the deformation behavior., with the following equation, $\sigma = K\epsilon^{n}$, where σ is true stress, ϵ is true strain, K is the strength hardening coefficient and n is the strength hardening exponent. Materials used in the simulations were drawn from [8]. Table 2 lists these properties.

Table (2): Material properties used in modeling

Mechanical properties	Rivet (2117 T4)	Sheets (2024 T4)
Young's Modulus (psi)	10.4E6	
Poisson ratio	0.33	0.33
Yield Strength (Ksi)	45	24
Hardening parameter	K=105.88Ksi n=0.1571	K=80Ksi n=0.15
Density (lb/in^3)	0.101	0.101

5.Results and dissection

The tensile strengths of the riveting sheet joints with forming forces of 10,12 and 30kN are shown in figure 3. The improved riveting shared with a forming force of 10 KN has the lowest tensile strength, while the riveting shared with a forming force of 12 and KN has the highest tensile strength. The tensile strength of the forming strength of 30 KN was 39.6% more than the forming strength of 10 KN.

Figure (3): Specimen and rivets after tensile strength test

For all models, a 10 KN preload is applied to tighten the joint and clamps the aluminum plates. Subsequently, a longitudinal tensile displacement of 1.5 mm was applied to the end of the middle plate through a quasi-static process. In figure 4, the load-displacement curves and local deformation of the hole obtained from the experiments and simulations were compared. For the experiments, the average values of three tests were presented. The maximum standard deviation load in samples SW1e1, SW1e2, and SW1e3 were found to be 10KN, 12KN, and 30KN, respectively. The figures show it the shear-out was the failure mode in the double bolt junctions, and the net tension was found to be the mode of failure.

Table (3): Shows the results of the experiment and ANSYS for a load of 10,12,30KN

Gap between sheets	ANSYS Result (m p stress)	Experimental Results (m p stress)
0.5 mm	334.92 (N/mm^2)	307.63 (N/mm^2)
1mm	267.93 (N/mm2)	244.12 (N/mm2)
1.5 mm	200.95 (N/mm2)	188.34 (N/mm2)

Figure 4,5 and figure 6 shows the load-displacement curves of double bolt joints in different specimens. The curves show that the joint is stronger than the individual bolts. It has generally been stated that more tensile force is required to achieve the same displacement. From the two joint specimens, it was found that DW1e1 needed a higher force to reach the same displacement as SW1e1. The difference between the versions of software was 40%. This study found that the double bolt junctions had greater load-carrying capacities. The different failure modes caused the location of the crack to be different in double bolt junctions.

Figures 4, 5 and figure 6 show how changing the width (W) and edge distance (e) affects the behavior of load-displacement curves. From figures 4, 5, and figure 6, It can be seen that an increase in the width of single-screw connections did not significantly affect the behavior of the connection under tensile load, while with the increase of e, the joint strength increased significantly. With increasing W from 9.5mm(1.5*d*) to 12.7 mm (2*d*) and 15.9 mm (2.5*d*), The maximum load for a displacement of 4 mm is increased by 23% and 37%, respectively (d is the bolt diameter).

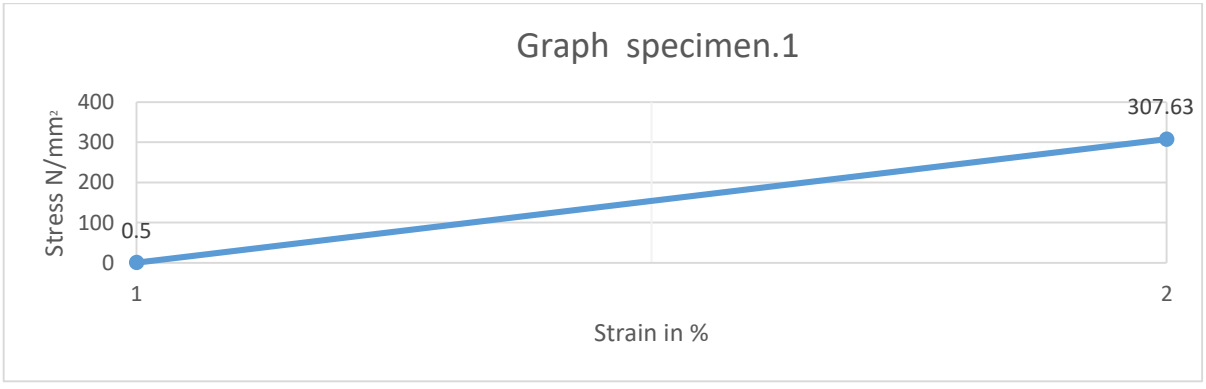

Figure (4): Shows the graph of stress-strain for a load of 10KN

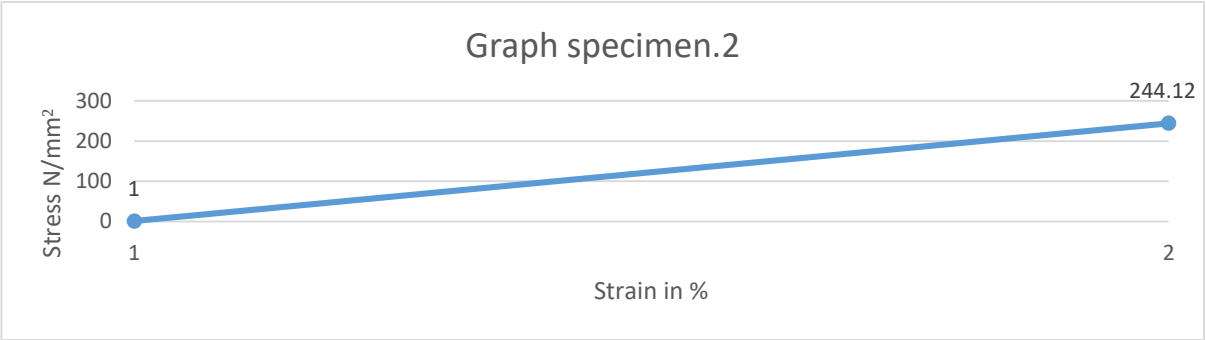

Figure (5): Shows the graph of stress-strain for a load of 12KN

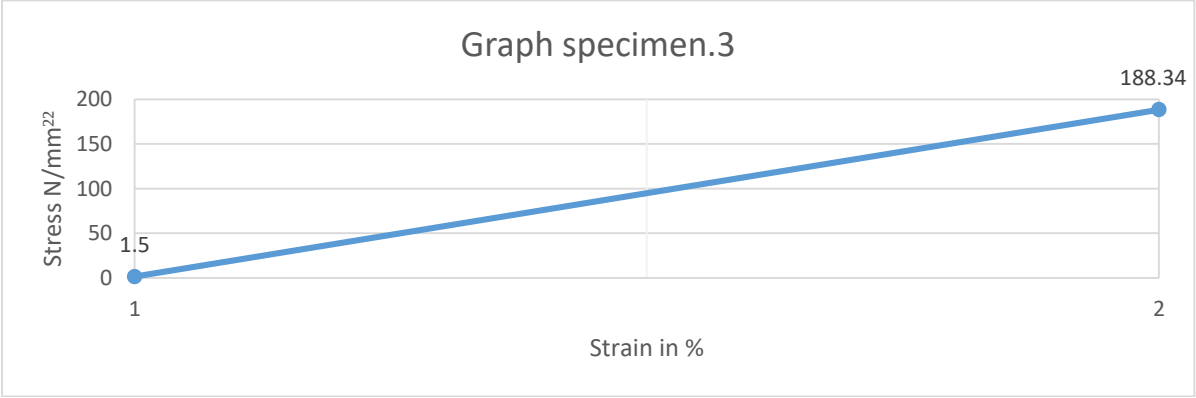

Figure (6): Shows the graph of stress-strain for a load of 30KN

6. Finite Element analysis version (16).

This package is used to carry out the analysis of the solid work of the riveting sheet. It gives accurate results for stress distribution with the tensile loads.

In Figures 7, 8, and 9, the distribution of stress von Mises on the circumference is plotted when the tensile load reaches 10 kN, 12KN, and 30 KN in the double bolt joints, respectively.

The line of tensile loads 10 kN,12, and 30 KN is specified in Figures 7,8, and 9. It can be realized from figures 7,8 and 9 that the KN initiation of cracks in the double bolt junctions was approximately at $2\pi/7$ rad (90°).

This was due to the difference in failure modes observed for the double bolt joints in experiments.

This observation was confirmed with stress results shown in Figures 7,8 and 9. In DW1e1 and DW2e1 and DW3e1 specimens, the maximum stress at the critical point reached almost the ultimate strength of the aluminum alloy plate. While in the other specimens under the same load, the stress, even at the critical point, was far from the ultimate strength but met the yield strength of the plate. For example, with increasing the load to 30 KN, the hole diameter of SW1e2 increased from 6.35 to 7.02 mm, confirming the occurrence of bearing failure mode.

Based on finite element stress results, net tension was found as the catastrophic failure mode for the double bolt joints (Figures 7, 8, and 9). this is evident in Figures 7,8 and 9 that in the

joints of the double bolt joints of DW1e1, DW1e2, and DW1e3, 30 KN was the maximum load required for these samples for the net-tension failure mode experiment (when the applied tensile load reached 30 KN, the net-tension failure occurred). Figure 9 also shows that von Mises narrows at the critical point of the hole in the above samples to meet the maximum tensile strength of the aluminum plate. Whereas, the specimens with a bigger W had only plastic deformations.

For instance, with an increasing load to 30 KN, the hole diameter of DW2e1 increased from 6.35 to 6.91 mm. Thus, the bearing failure mode occurred in these specimens. Figures 7,8 and 9 show von Mises stress lines in the middle panel of all the joints of the twin screws, respectively.

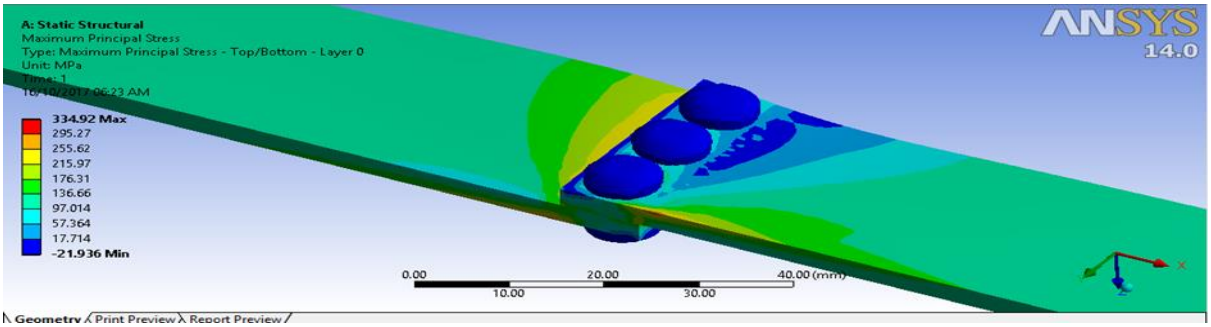

Figure (7): ANSYS finite element model of 10KN load

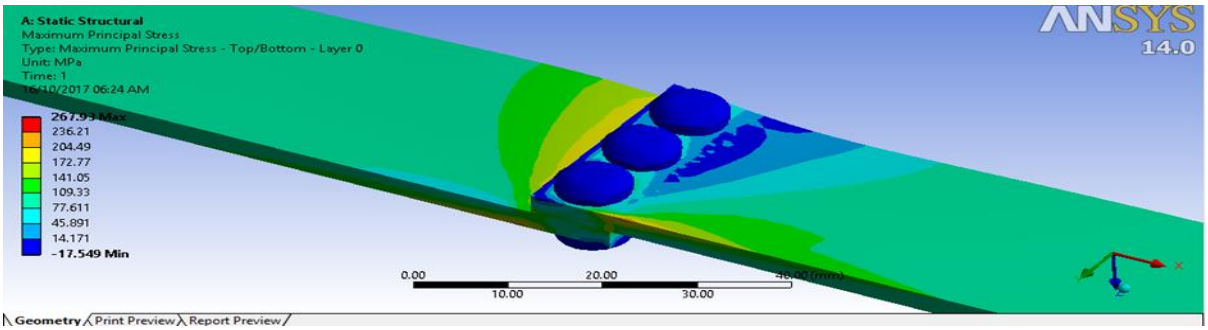

Figure (8): ANSYS finite element model of 12KN load.

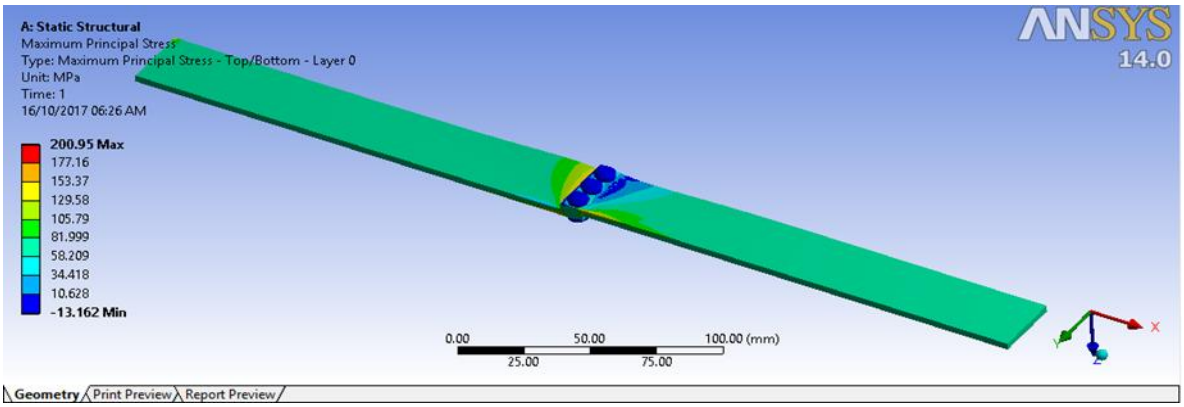

Figure (9): ANSYS finite element model of 30KN load.

7. Gap between sheets.

In this study, the observed results obtained from the experimental and finite element ANSYS were analyzed. A smaller gap increase stress it increases the strength of the lap joint when the gap between sheets it's bigger the stress decreases when the gap between sheets increases causing the amount of material growth between sheets and bulging on sheets, leads loose of the joint to failure of lap joint. The gap between the leaves should be as small as possible, a smaller gap between the leaves keeps residual stress low to give the quality of riveted lap subscribed to this study maximum allowable gap between the leaves it's 0.5mm the amount of material growth increases with an increase the hole between the sheets.

Table (4): Specimen details (for sequences 1 3 2)

Sequences number	Gab between sheet	Margin (m=1.5d)	Pitch (p =3d)	Pitch (p =4d)	Pitch (p =5d)
1	0.5mm	4.8	9.6	12.8	16
2	1mm				
3	1.5mm				

Table (5): Shows the relation between the experiment and finite element ANSYS and the gap between the sheet.

Gap between sheets	Ansys Result (m p stress)	Experimental Results (m p stress)
0.5 mm	334.92 (N/mm2)	307.63 (N/mm2)
1 mm	267.93 (N/mm2)	244.12 (N/mm2)
1.5 mm	200.95 (N/mm2)	188.34 (N/mm2)

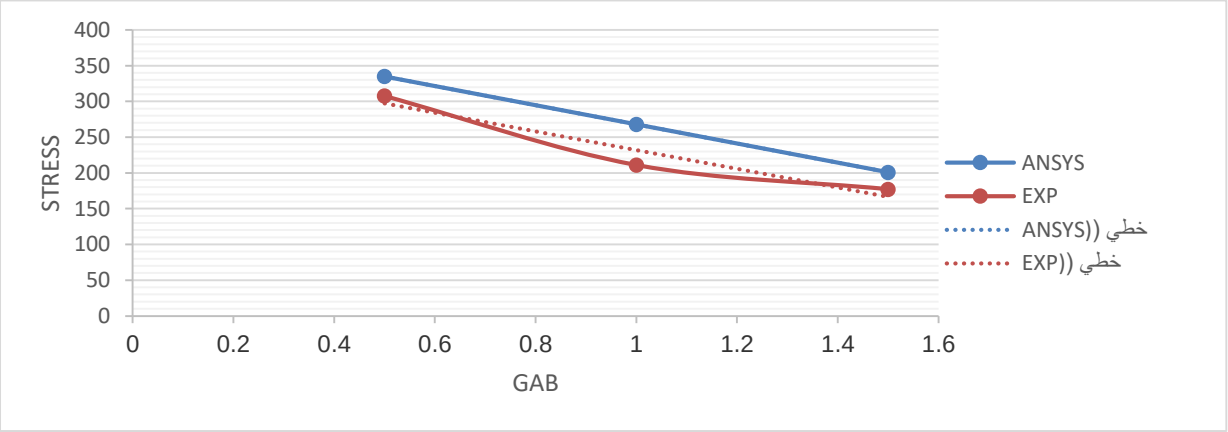

Figure (10): Shows the relationship between the experiment and finite element ANSYS and the gap between the sheet.

Figure 10 explain the relationship between the results obtained from the experiment, the ANSYS finite element, and the gap between the sheet. It illustrates that as the gap increases the stresses for both the experiment and the finite element ANSYS decreases.

Table (6): Shows the experiment and ANSYS for a load of 12KN

Gap between sheets	ANSYS Result (m p stress)	Experimental Results (m p stress)
1 mm	1004.7 (N/mm2)	711.34 (N/mm2)
1,5 mm	468.88 (N/mm2)	300.87 (N/mm2)
2 mm	401.9 (N/mm2)	203.03 (N/mm2)

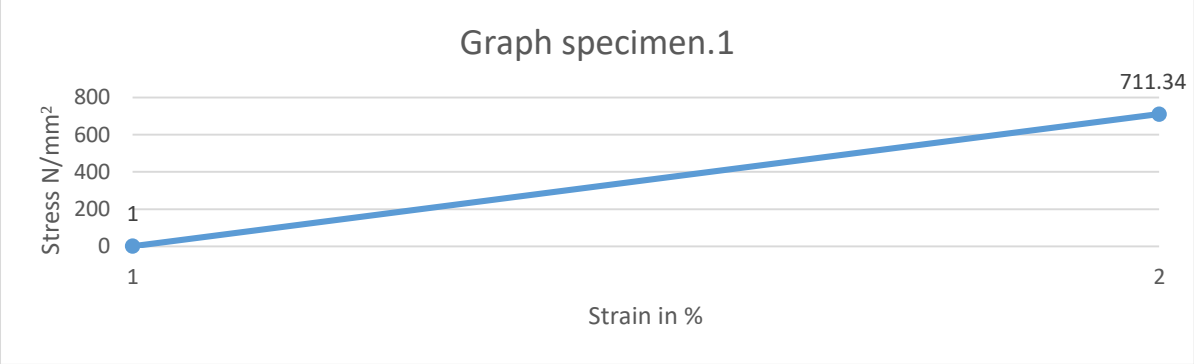

Figure (11): Shows the graph of stress-strain for a load of 10KN

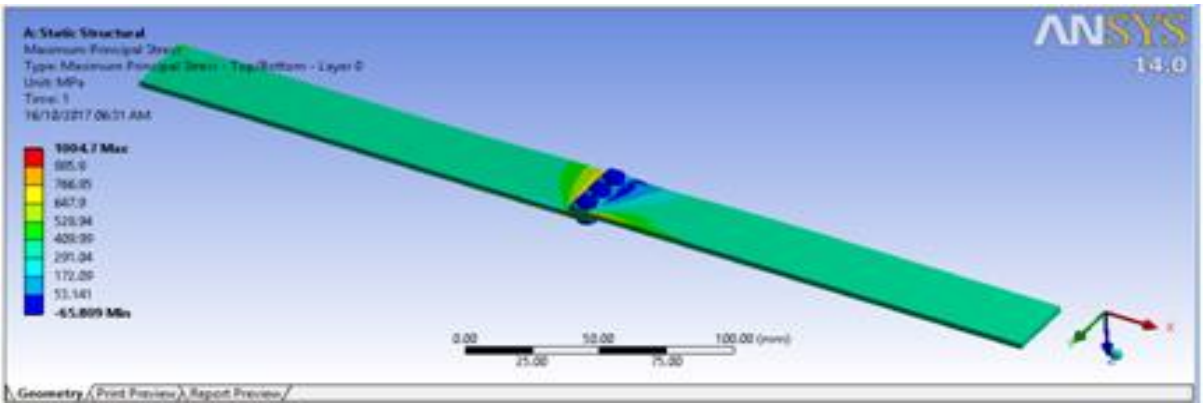

Figure (12): ANSYS finite element model of 10KN load

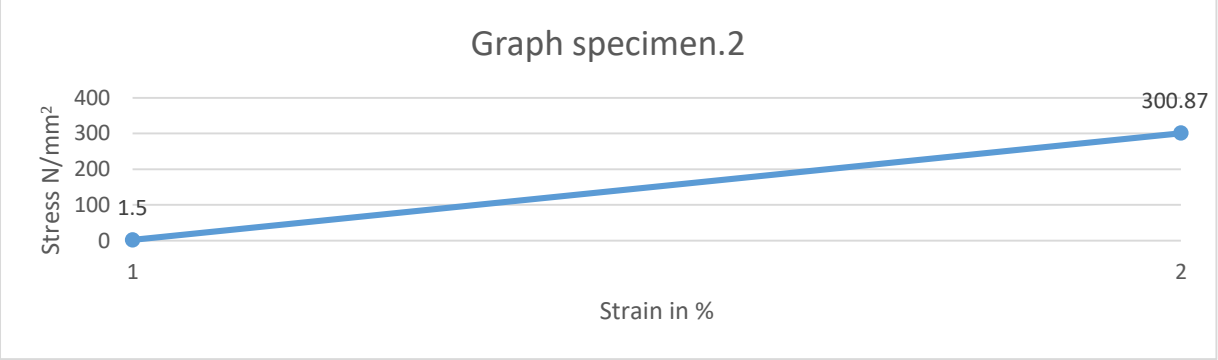

Figure (13): Shows the graph of stress-strain for a load of 12KN

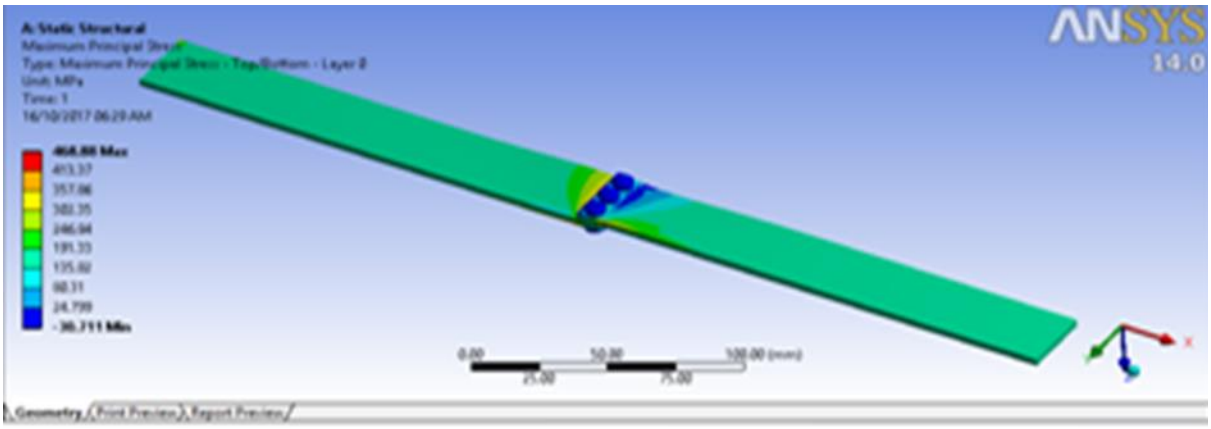

Figure (14): ANSYS finite element model of 12KN load

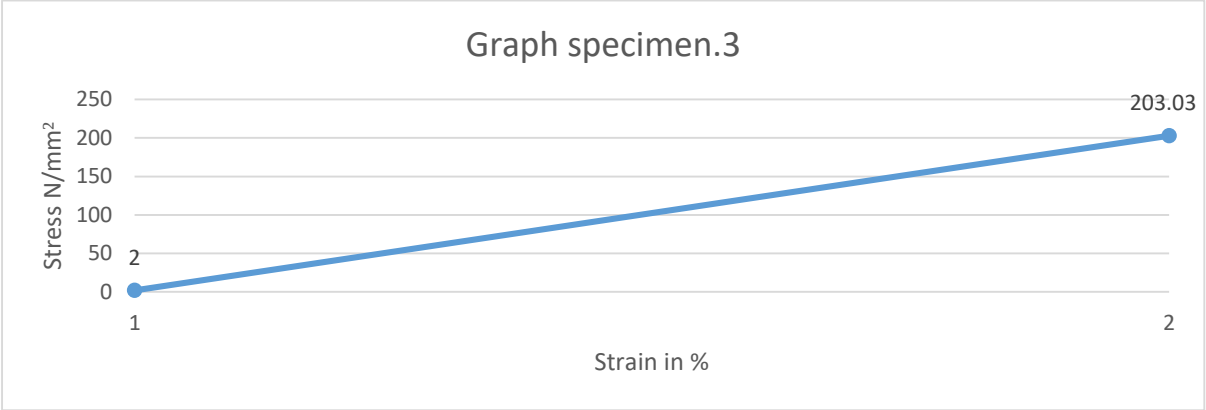

Figure (15): Shows the graph of stress-strain for a load of 30KN

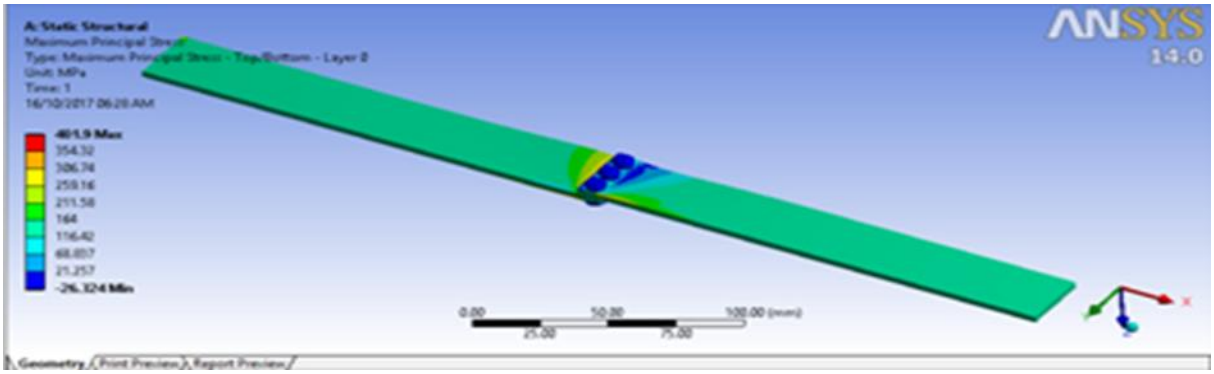

Figure (16): ANSYS finite element model of 30KN load

Figure 17 shows the relationship between the results obtained from the experiment and finite element ANSYS and the gap between the sheet. It illustrates that as the load increases the stresses for both the experiment and the finite element ANSYS decreases.

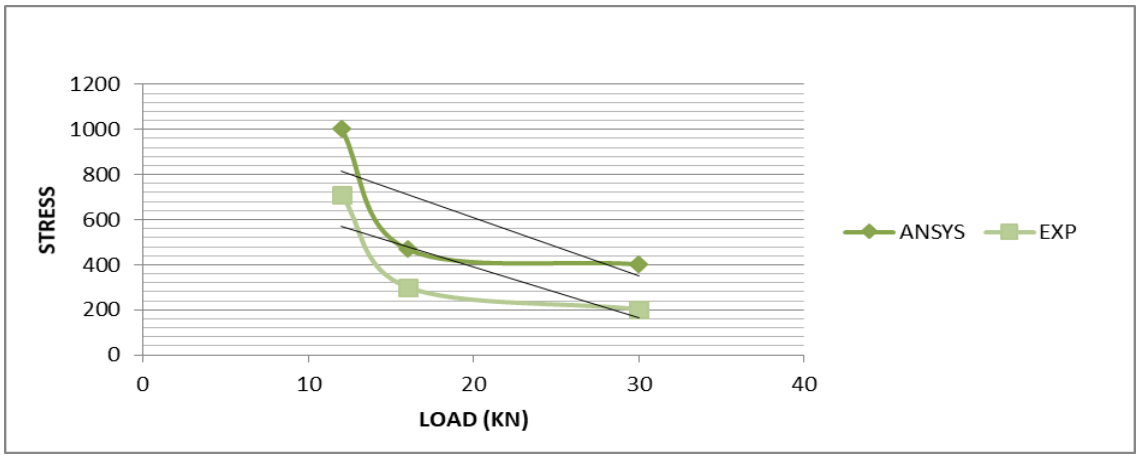

Figure (17): Shows the relationship between the shear stress and load for the experiment and finite element ANSYS

8. Distance between Rivets.

In specimens No7,8,9 it is observed that the shear stress is nearest between experimental and ANSYS results. Experimental results highlighted that as the pitch increases at a different pitch of joint it increases the shear strength of the joint. As compared with Ansy's result that also shows increasing in joint strength by increasing the pitch and thickness of the plate. When increased pitch between rivets, increases the amount of material growth. When the pitch is bigger, the residual stress is better, and when the pitching is smaller, the residual stress becomes bigger.

Table (7): Shows the relation between the experiment and finite element ANSYS and the pitch between the rivet.

Pitch between rivets	Ansys Result (M Shear Stress)	Experimental Results (M Shear Stress)
9.6 mm	113.29(N/mm2)	123.88(N/mm2)
12.8 mm	151.05(N/mm2)	172.11N/mm2)
16mm	188.81(N/mm2)	195.17 (N/mm2)

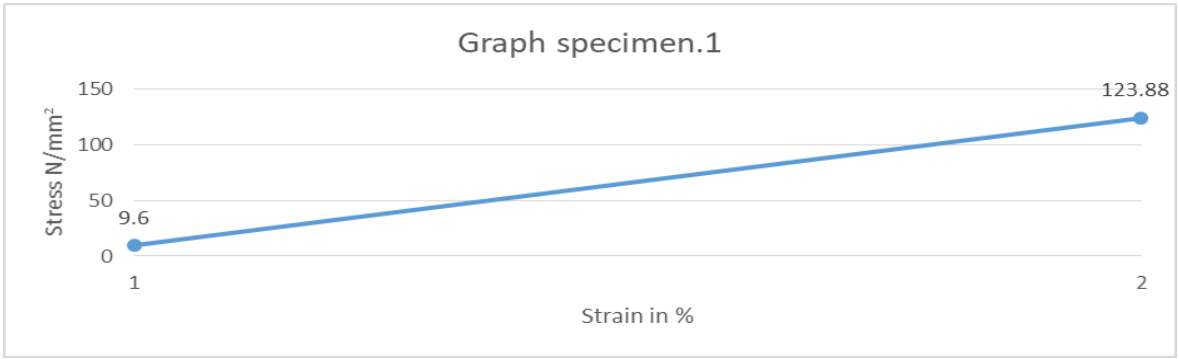

Figure (18): Shows the graph of stress-strain for a load of 10KN

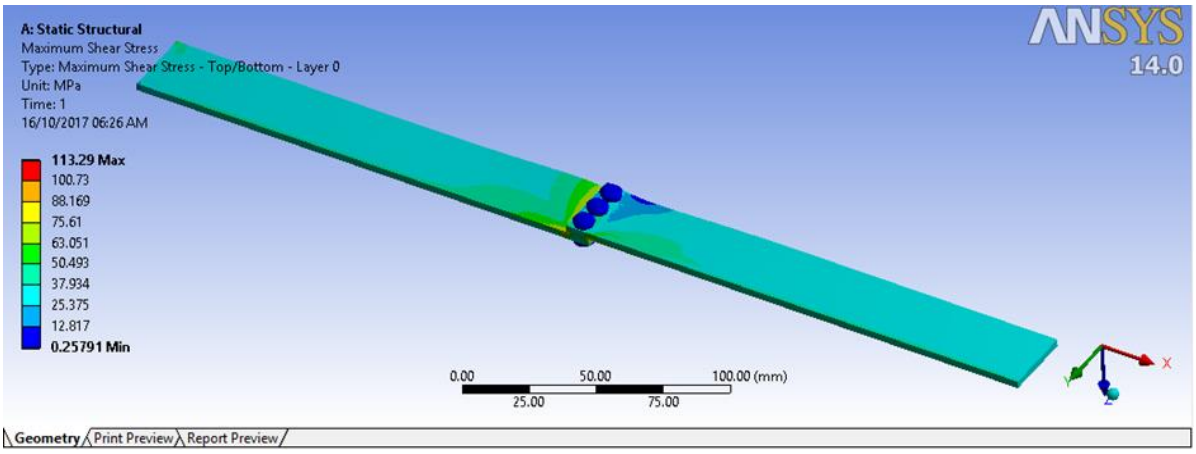

Figure (19): ANSYS finite element model of 10KN load

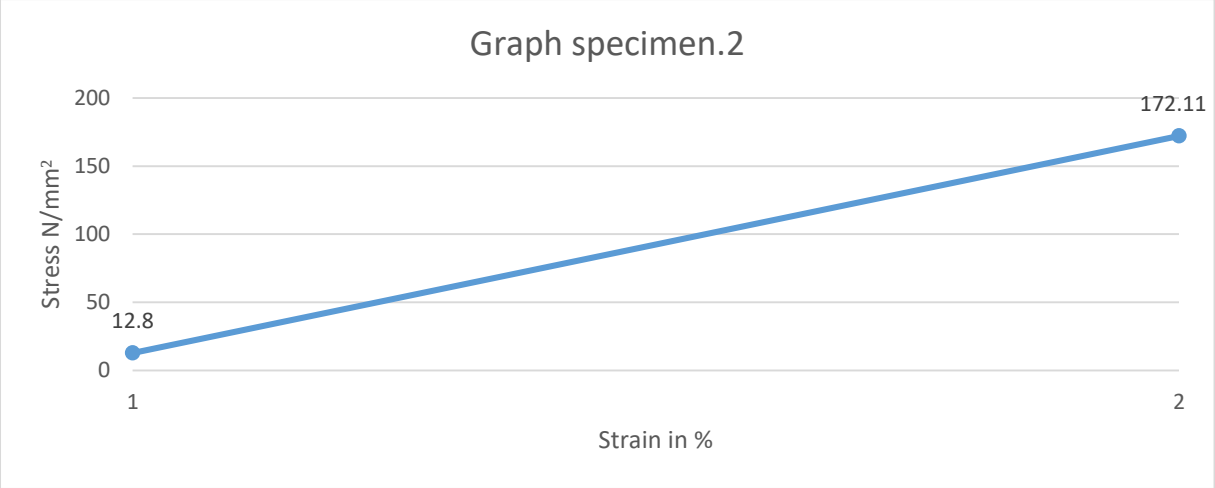

Figure (20): Shows the graph of stress strain for a load of 12KN

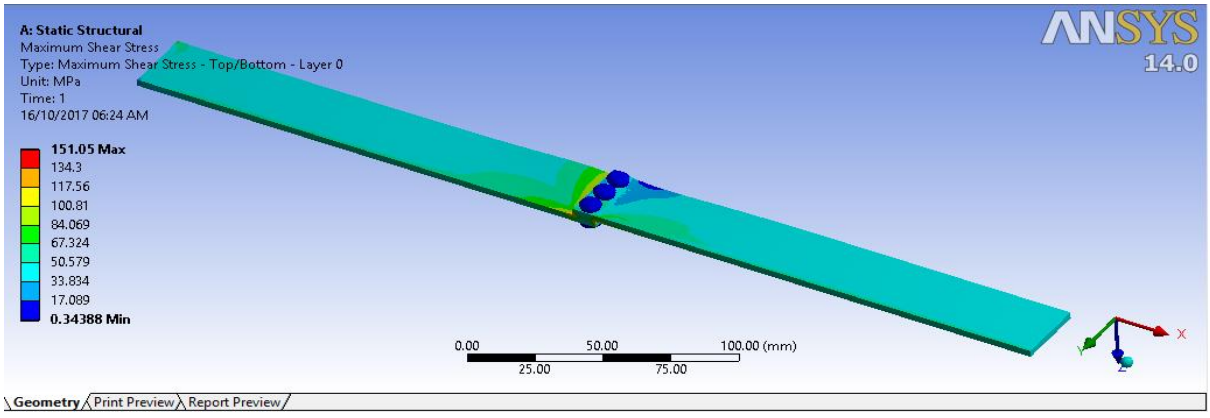

Figure (21): ANSYS finite element model of 12KN load

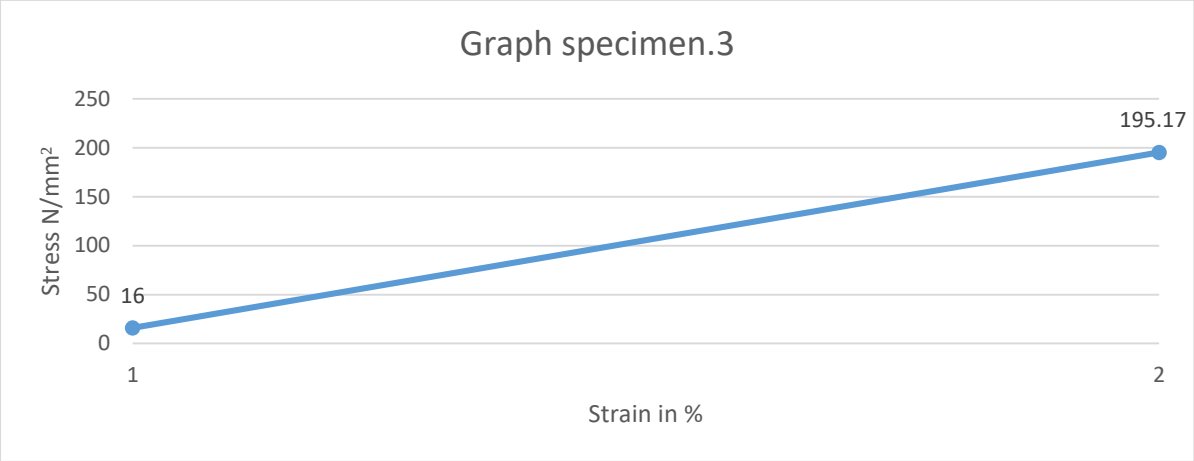

Figure (22): Shows the graph of stress strain for a load of 30KN

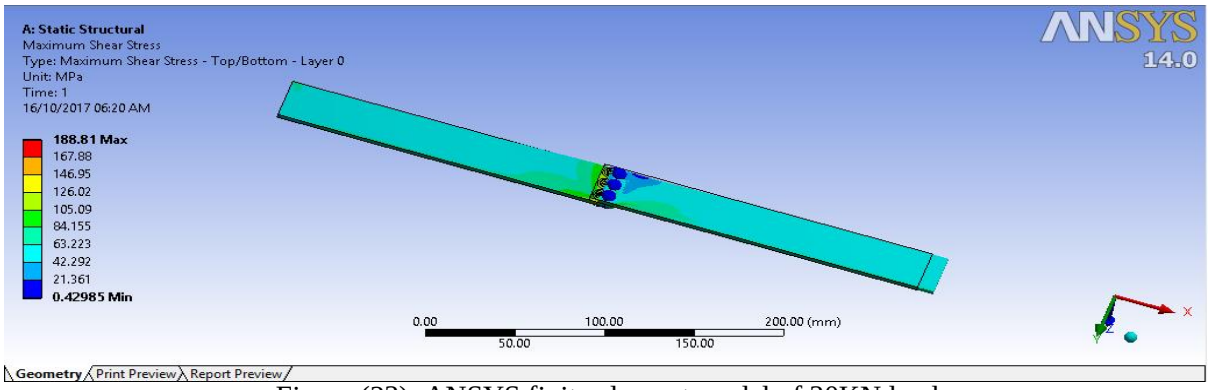

Figure (23): ANSYS finite element model of 30KN load

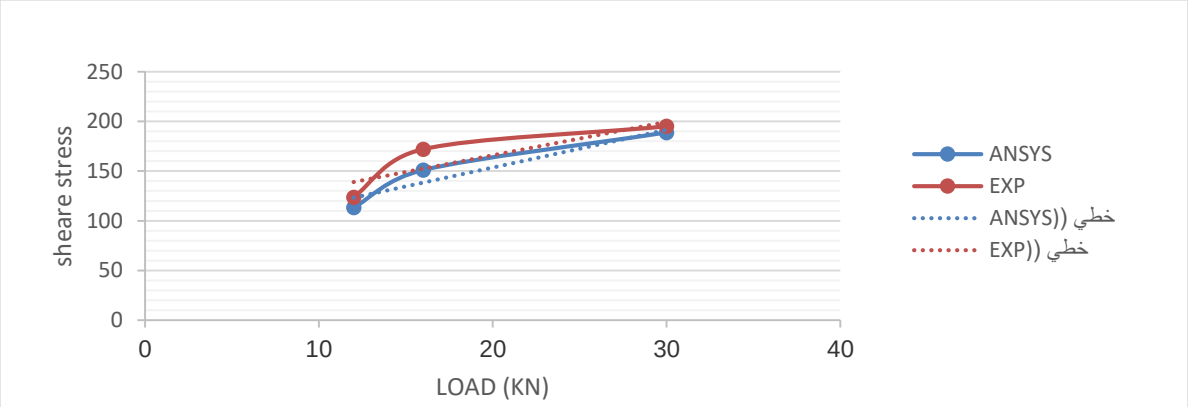

Figure (24): Shows the relationship between the shear stress and load for experiment and finite element ANSYS.

Figure 24 illustrates the obtained results from the experiment and finite element ANSYS and the relation between them and also the gap between the sheet. It illustrates that as the load increases the stresses for both the experiment and the finite element ANSYS increase.

9. Conclusion.

From this study the following conclusions have been obtained: -

Experiment and finite element model were developed to predict the tensile behavior of Al 2024-T4 double-lap bolted joints with double fasteners. The model was verified by experimental tests and there was a good agreement between the experimental and numerical results.

1. Shear-out was the dominant failure mode in the net-tension failure mode that occurred in the double bolt junctions.
2. The study shows that the bolt of double junctions gives a large load capacity under the tensile loading. They resist loads 40%–49% magnitude high. The initiation of failure in the double bolt junctions occurred at the critical edge of the hole where there is a high-stress concentration ($\pi/2$ rad); while in the single bolt joints the initiation of failure occurred at $2\pi/7$ rad.
3. In the double bolt joints, changing *e* had almost no effect on the tensile behavior of the joint. However, increasing *W* from 25.4 to 30 mm increased the load carrying capacity by 28%.

References

[1] Chen, Chao, Yawen Ouyang, and Denglin Qin. "Finite element analysis of material flow in flat-rivet clinching process." The International Journal of Advanced Manufacturing Technology 116, no. 5 (2021): 1961-1974.

[2] Deng, Jiang-Hua, Feng Lyu, Ru-Ming Chen, and Zhi-Song Fan. "Influence of die geometry on self-piercing riveting of aluminum alloy AA6061-T6 to mild steel SPFC340 sheets." Advances in Manufacturing 7, no. 2 (2019): 209-220.

[3] Falck, Rielson, Jorge F. Dos Santos, and Sergio T. Amancio-Filho. "Microstructure and mechanical performance of additively manufactured aluminum 2024-t3/acrylonitrile butadiene styrene hybrid joints using an addjoining technique." Materials 12, no. 6 (2019): 864.

[4] Hönsch, Florian, Josef Domitner, Christof Sommitsch, and Bruno Götzinger. "Modeling the failure behavior of self-piercing riveting joints of 6xxx aluminum alloy." Journal of Materials Engineering and Performance 29, no. 8 (2020): 4888-4897.

[5] Makwana, Alpesh H., and A. A. Shaikh. "Performance assessment and optimization of hybrid composite patch repair of aircraft structure." Multidiscipline Modeling in Materials and Structures (2020).

[6] Pramanik, A., A. K. Basak, Yu Dong, P. K. Sarker, M. S. Uddin, G. Littlefair, A. R. Dixit, and S. Chattopadhyaya. "Joining of carbon fibre reinforced polymer (CFRP) composites and aluminium alloys–A review." Composites Part A: Applied Science and Manufacturing 101 (2017): 1-29.

[7] Sripunchat, Teerawut, and Komson Jirapattarasilp. "Effect of Riveting Parameters on Strength of Aluminium Joint." In Advanced Materials Research, vol. 650, pp. 616-622. Trans Tech Publications Ltd, 2013.
[8] Schwinn, Julian, Eric Breitbarth, Thomas Beumler, and Guillermo Requena. "Blunt Notch Strength of AA2024 3-3/2-0.4 Fibre Metal Laminate Under Biaxial Tensile Loading." Metals 9, no. 4 (2019): 413.
[9] Thurston, Brian P., Daniel R. Klenosky, Heath E. Misak, Anupam Vivek, and Glenn S. Daehn. "Small-Scale Impact Welding of High-Strength Aluminum Alloys: Process and Properties." Journal of Materials Engineering and Performance (2022): 1-14.
[10] Uhe, Benedikt, Clara-Maria Kuball, Marion Merklein, and Gerson Meschut. "Improvement of a rivet geometry for the self-piercing riveting of high-strength steel and multi-material joints." Production Engineering 14, no. 4 (2020): 417-423.
[11] Ying, Liang, Tianhan Gao, Minghua Dai, Ping Hu, and Jingchao Dai. "Towards joinability of thermal self-piercing riveting for AA7075-T6 aluminum alloy sheets under quasi-static loading conditions." International Journal of Mechanical Sciences 189 (2021): 105978.
[12] Zeng, Chao, Jiu Tian Xue, Xiang Yao Liu, and Wei Tian. "Design variables influencing the fatigue of Al 2024-T3 in riveted aircraft lap joints: Squeeze force and initial fit tolerance." International Journal of Fatigue 140 (2020): 105751.